

New lipophilic 3-hydroxy-4-pyridinonate iron(III) complexes: synthesis and EXAFS structural characterisation†

Walkiria Schlindwein,^a Emma Waltham,^b John Burgess,^b Norman Binsted,^c Ana Nunes,^d Andreia Leite^e and Maria Rangel^{*e}

Received 8th July 2005, Accepted 27th October 2005

First published as an Advance Article on the web 22nd November 2005

DOI: 10.1039/b509671e

New tris-iron(III) chelates of 3-hydroxy-4-pyridinone ligands derived from maltol (3-hydroxy-2-methyl-4-pyrone) or ethylmaltol (2-ethyl-3-hydroxy-4-pyrone), including a variety of *N*-aryl (phenyl, 4'-tolyl, 4'-(*n*-butyl)phenyl, 4'-(*n*-hexyl)phenyl) and *N*-benzyl (4'-methylbenzyl, 4'-fluorobenzyl and 4'-(trifluoromethyl)benzylamine) substituents on the nitrogen atom of the pyridinone ring, have been prepared. Characterization by C,H,N elemental analysis and thermogravimetric measurements indicates that most of the complexes are obtained as hydrates of general formula $ML_3 \cdot xH_2O$. Structural characterization of these difficult to crystallize lipophilic complexes has been achieved by EXAFS spectroscopy. Solutions of iron(III) complexes of maltol, ethylmaltol, 1,2-dimethyl-3-hydroxy-4-pyridinone and 1-phenyl-2-methyl-3-hydroxy-4-pyridinone in methanol–water mixtures were also examined by EXAFS. Distances from the central atom to ligand atoms, within 6 Å of the metal, have been determined in the solid and solution samples and the results show that the structure observed in the powder is maintained in solution. The local structure around the metal centre, bond distances and bond angles, does not change significantly with variable lipophilicity, thus indicating that ligands may be tailored according to specific needs without altering their chelation properties. EXAFS data analysis for this set of tris-iron(III) compounds illustrates the important contribution of both intra-ligand and inter-ligand multiple scattering pathways through the metal centre to a peak observed in the FT spectrum at twice the metal–ligand distance (~4 Å). The present results demonstrate that EXAFS features at twice the metal–ligand distance are valuable in the assignment of molecular geometry and that location of hydration water molecules, by EXAFS analysis, is limited by the geometry of the complexes, in particular for those in which ligands containing phenyl rings are present.

Introduction

Ligands of the 3-hydroxy-4-pyrone and 3-hydroxy-4-pyridinone types are well known, mainly by reason of their biomedical applications.^{1–19} The 3-hydroxy-4-pyrones maltol and ethylmaltol have the pharmacological advantage of being permitted food additives²⁰ and the closely related 3-hydroxy-4-pyridinones are particularly attractive for pharmaceutical purposes since their structure allows tailoring of their hydrophilic/lipophilic balance (HLB),²¹ without significantly changing its chelating properties. Variations in HLB can be achieved by simply introducing appropriate substituents on the endocyclic nitrogen atom of the pyridinone ring, the 3-hydroxy-4-pyridinones are synthesized by the reaction of 3-hydroxy-4-pyrones with primary amines, thus leading to the optimal lipophilicity for delivery or removal of metal ions in

the human body.²² As this synthetic approach, under appropriate conditions, works for almost any primary amine a very wide range of 1-substituted-3-hydroxy-4-pyridinones can be prepared,²³ from hydrophilic when sulfonate- or carboxy-groups²⁴ are incorporated to very lipophilic when the substituent on the ring-nitrogen is a long alkyl chain or an alkyl-substituted phenyl or benzyl group. Substituted benzyl groups provide a means of varying the ligand's HLB while having very little effect on its donor properties and thus on stabilities of its complexes.²⁵ F- or CF₃-for-H substitution provides another useful approach to modifying the HLB of ligands and complexes. The excellent chelating properties exhibited by the 3-hydroxy-4-pyridinone ligands towards M(III) and M(II) metal ions, in conjunction with the possibility of synthesizing strongly lipophilic derivatives, also makes this class of ligands useful in the fields of analytical and environmental chemistry. 1-Phenyl- and 1-(4'-tolyl)-3-hydroxy-4-pyridinones have been assessed as reagents for the spectrophotometric determination of, *inter alios*, Fe(III),^{26,27} Ti(IV),²⁸ V(V)²⁹ and Nb(V).³⁰ Some 1-aryl-3-hydroxy-4-pyridinone derivatives have been demonstrated to be effective as extractants, from aqueous media, for a variety of metals such as Ga(III),³¹ Fe(III),³² Hf(IV),³³ Zr(IV),³⁴ Nb(V),³⁵ Ta(V)^{36,37} and U(VI).³⁸ In many cases effective metal ion separations have been achieved.

In continuance of our program of synthesis and solvation studies of complexes of substituted 1-aryl-3-hydroxy-4-pyridinones

^aLeicester School of Pharmacy, De Montfort University, Leicester, UK LE1 9BH

^bDepartment of Chemistry, University of Leicester, Leicester, UK LE1 7RH
^cHampshire, UK SO51 78HT

^dREQUIMTE, Departamento de Química, Faculdade de Ciências, Universidade do Porto, Portugal

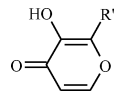
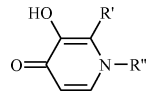
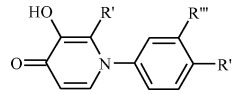
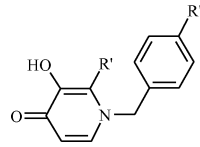
^eREQUIMTE, Instituto de Ciências Biomédicas de Abel Salazar, Universidade do Porto, Portugal. E-mail: mcrangel@fc.up.pt

† Electronic supplementary information (ESI) available: Colour version of Fig. 1. See DOI: 10.1039/b509671e

with fluorinated substituents such as $1\text{-CH}_2\text{CF}_3$ ³⁹ or with long alkyl chains as phenyl substituents⁴⁰ we now report the synthesis and characterization of novel iron(III) complexes with a variety of aryl (4'-(*n*-butyl)phenyl, 4'-(*n*-hexyl)phenyl and 4'-methoxyphenyl) and benzyl (benzyl, 4'-methylbenzyl, 4'-fluorobenzyl and 4'-(trifluoromethyl)benzylamine) substituents on the nitrogen atom of the pyridinone ring. The ligands and complexes in the present study are predominantly lipophilic and those containing long-chain substituents exhibit high solubilities in alcohols and are sparingly soluble or essentially insoluble in water. Consequently the compounds are relatively unsuitable for medical use, but suitable as metal extractants. Formulae and abbreviations are given in Table 1.

High lipophilicity makes crystallisation very difficult and for the majority of the reported compounds no suitable crystals for X-ray diffraction (XRD) were, or are likely to be, obtained. We have therefore used EXAFS spectroscopy to gain information on the local structure around the metal centres in the new complexes in the solid state and for some compounds in solution. From the chemical point of view, knowledge on the types of species formed upon solubilization or on solvation properties is very important as most of the compounds are active in solution. In our first study on this class of compounds we reported the presence and location of water molecules in the solid compounds and in solution based on the fitting of a peak at about 4 Å using the EXCURV92 code for EXAFS analysis.⁴¹ In this work, the number of multiple scattering paths was quite limited, being restricted to intra-ligand paths with only two different scattering atoms. Subsequent work has shown that the contribution of multiple scattering contributions involving three or more scattering atoms, and inter-ligand paths involving the first coordination shell are also important, and the origin of shells at approximately twice the first shell metal–ligand distance in the EXAFS Fourier transform (FT) has been the object of discussion in the literature.^{42–47} General agreement is that contributions from the shorter inter-ligand and all the intra-ligand multiple scattering pathways should be included in order to assess the significance of solvation molecules.

Table 1 Formulae and abbreviation of the Fe(III) complexes studied

	Pyrones R' = CH ₃ ; Fe(ma) ₃ R' = C ₂ H ₅ ; Fe(ma) ₃
	Alkyl pyridinones R' = CH ₃ , R'' = H; Fe(mpp) ₃ R' = CH ₃ , R'' = CH ₃ ; Fe(dmpp) ₃
	Phenyl pyridinones R' = CH ₃ , R'' = R''' = H; Fe(ppp) ₃ R' = C ₂ H ₅ , R'' = CH ₃ , R''' = H; Fe(pbtpp) ₃ R' = CH ₃ , R'' = C ₄ H ₉ ; R''' = H; Fe(pbp) ₃ R' = C ₂ H ₅ , R'' = C ₄ H ₉ ; R''' = H; Fe(epb) ₃ R' = CH ₃ , R'' = C ₉ H ₁₃ , R''' = H; Fe(phpp) ₃
	Benzyl pyridinones R' = C ₂ H ₅ , R'' = CF ₃ ; Fe(etb) ₃ R' = C ₂ H ₅ , R'' = F; Fe(efb) ₃ R' = CH ₃ , R'' = CH ₃ ; Fe(embb) ₃

In the present work we report the local structure around the iron atom for a new set of hydrated 3-hydroxy-4-pyridinone iron(II) complexes using a more rigorous multiple scattering analysis. Previously we used a restrained refinement procedure (soft restraints).⁴⁸ However, we found little deformation of the ligand during refinement, and essentially the same results could be obtained using constrained refinement, in which the ligand defined by the crystal structure was moved as a rigid body. This rather simpler approach was adopted here.

Experimental

Materials

All chemicals were reagent grade and were used as received unless otherwise specified. Sources: Fe(NO₃)₃·6H₂O (Merck), maltol (3-hydroxy-2-methyl-4-pyrone, Aldrich), ethylmaltol (2-ethyl-3-hydroxy-4-pyrone, Pfizer or Aldrich), aniline (Aldrich), 4-toluidine (Aldrich), 4-anisidine (Aldrich), 4-(*n*-butyl)aniline (Aldrich), 4-(*n*-hexyl)aniline (Aldrich), benzylamine (Sigma), 4-methylbenzylamine (Sigma), 4-fluorobenzylamine (Aldrich or Sigma) and 4-(trifluoromethyl)benzylamine (Sigma). Methanol was Merck, PA grade; water was deionized. The 3-hydroxy-4-pyridinone ligands were synthesized and purified as previously described.^{49–51}

Physical techniques

IR spectra were recorded (KBr pellets) in the range 4000–400 cm⁻¹ using a Perkin-Elmer 580B spectrometer. Fast atom bombardment (+FAB) spectra were obtained using a Kratos concept double-focusing mass spectrometer. ¹H NMR spectra were recorded in CD₂Cl₂ with a Bruker AX 250 MHz spectrometer. Elemental analysis were performed at the Microanalytical Laboratory, Department of Chemistry, University of Manchester and at Butterworth Laboratories Ltd., Teddington, UK. Thermogravimetric spectra have been obtained on a TA Instruments Thermal Analyst 2000, TGA 50 Thermogravimetric Analyzer.

Synthesis and characterization of metal complexes

Iron(III) complexes of general formula, ML₃·xH₂O (L = 3-hydroxy-4-pyridinone), were prepared by a method analogous to that established in the literature for aluminium(III) complexes of this type.⁵² Aqueous or ethanolic solutions of the corresponding metal nitrates were stirred with an ethanolic solution of the ligand (in a 1 : 3 stoichiometric amount) and the pH was adjusted to 8 using an aqueous solution of sodium hydroxide. The solids were filtered, re-crystallized from ethanol–water and kept over P₂O₅. All compounds were characterized by C,H,N elemental analysis, mass spectrometry, FTIR and ¹H NMR and TGA analysis; we report below the results obtained for the new compounds, which are all deep red–brown in color. The number of hydration molecules was calculated according to EA results and percentage of weight loss determined from TGA analysis.

Tris (1-phenyl-3-hydroxy-2-methyl-4-pyridinonato) iron (III), Fe(ppp)₃·2H₂O. (Found: C, 62.04; H, 4.94; N, 5.92. Calc. for C₃₆H₃₄N₃O₈Fe: C, 62.44; H, 4.95; N, 6.07%), FAB-MS: *m/z* 657 [ML₃H]⁺; 457 [ML₂H]⁺; 257 [MLH]⁺, IR: 1492, 1505, 1538, 1589, 3200–3600 cm⁻¹.

Tris(1-(4'-tolyl)-3-hydroxy-2-ethyl-4-pyridinonato)iron(III), Fe(eptp)₃·2.5H₂O. (Found: C, 64.51; H, 5.92; N, 5.27. Calc. for C₄₂H₄₇N₃O_{8.5}Fe: C, 64.21; H, 6.03; N, 5.35%), FAB-MS: *m/z* 693 [ML₃H]⁺; 465 [ML₂H]⁺; 237 [MLH]⁺ IR: 1398, 1496, 1556, 1600, 3200–3600 cm⁻¹.

Tris(1-(4'-butyl)phenyl-3-hydroxy-2-methyl-4-pyridinonato)iron(III), Fe(pbpp)₃·H₂O. (Found: C, 68.76; H, 6.88; N, 5.07. Calc. for C₄₈H₅₆N₃O₇Fe: C, 68.34; H, 6.64; N, 5.07%). FAB-MS: *m/z* 825 [ML₃H]⁺; 569 [ML₂H]⁺; 313 [MLH]⁺, IR: 1468, 1508, 1541, 1589, 3200–3600 cm⁻¹.

Tris(1-(4'-butyl)phenyl-3-hydroxy-2-ethyl-4-pyridinonato)iron(III), Fe(epbpb)₃·H₂O. (Found: C, 69.79; H, 7.06; N, 4.90. Calc. for C₅₁H₆₂N₃O₇Fe: C, 69.16; H, 7.01; N, 4.75%). FAB-MS: *m/z* 867 [ML₃H]⁺; 597 [ML₂H]⁺; 327 [MLH]⁺, IR: 1470, 1508, 1537, 1587, 3200–3600 cm⁻¹.

Tris(1-(4'-hexyl)phenyl-3-hydroxy-2-methyl-4-pyridinonato)iron(III), Fe(phpp)₃·H₂O. (Found: C, 69.82; H, 7.49; N, 4.52. Calc. for C₅₄H₆₈N₃O₇Fe: C, 69.90; H, 7.33; N, 4.53%). FAB-MS: *m/z* 909 [ML₃H]⁺; 625 [ML₂H]⁺; 341 [MLH]⁺, IR: 1468, 1508, 1541, 1590, 3200–3600 cm⁻¹.

Tris(1-(4'-fluoro)benzyl-3-hydroxy-2-ethyl-4-pyridinonato)iron(III), Fe(efbpb)₃·2H₂O. (Found: C, 60.63; H, 5.03; N, 5.11. Calc. for C₄₈H₆₀N₃O₈Fe: C, 60.72; H, 5.23; N, 5.06%). FAB-MS: *m/z* 795 [ML₃H]⁺; 548 [ML₂H]⁺; 302 [MLH]⁺, IR: 1585, 1535, 1505, 1490, 3200–3600 cm⁻¹.

Tris(1-(4'-methyl)benzyl-3-hydroxy-2-ethyl-4-pyridinonato)iron(III), Fe(embpb)₃·3H₂O. (Found: C, 64.24; H, 6.33; N, 4.98. Calc. for C₄₈H₆₂N₃O₉Fe: C, 64.58; H, 6.52; N 5.02%). FAB-MS: *m/z* 783 [ML₃H]⁺; 540 [ML₂H]⁺; 298 [MLH]⁺, IR: 1590, 1535, 1510, 1495, 3200–3600 cm⁻¹.

Tris(1-(4'-trifluoromethyl)benzyl-2-ethyl-3-hydroxy-4-pyridinonato)iron(III), Fe(etbpb)₃·3H₂O. (Found C, 55.74; H, 4.22; N, 4.37. Calc. for C₄₈H₆₂N₃O₉Fe: C, 56.14; H, 4.38; N, 4.36%). FAB-MS: *m/z* 945 [ML₃H]⁺; 648 [ML₂H]⁺, IR: 1610, 1535, 1535, 1490, 3200–3600 cm⁻¹.

EXAFS data collection

EXAFS experiments were performed in the region of the Fe K-edge using station 7.1 at the Synchrotron Radiation Source, Daresbury Laboratory. The beam energy was 2 GeV and a typical average stored ring current was 120 mA in multibunch mode and high-brightness lattice configuration. The energy calibration was done with a metal foil (Fe) before the start of the beamtime and re-checked after each new beam. Data were acquired in the EXAFS transmission mode, with argon-filled ion chambers using a Si(111) double crystal monochromator with 50% harmonic rejection.

Powder samples were prepared in the form of homogeneous pellets (~100 μm of thickness) and diluted with boron nitride when necessary. The solution samples used for the EXAFS experiments were saturated solutions of the complexes (0.08 mol dm⁻³) in a 20 : 80% (v/v) water–methanol mixture—the complexes are more soluble in methanol-rich mixtures than in methanol or water. The solution samples were analyzed in 2 mm thick liquid cells. All the experiments were carried out at room temperature and no sample

decomposition was observed after irradiation of multiple scans (average of three scans per sample).

EXAFS data analysis

EXAFS spectra were reduced to absorption vs. photon energy and background subtracted using the program PAXAS⁵³ and the most recent available version of EXCURVE (version 9.274) was used for curve fitting.

For both Fe(ma)₃ and Fe(dmpp)₃, an excellent fit was obtained using the published crystal structure,^{54,55} with refined values of the energy zero *E*_i, and either three or four groups of Debye–Waller terms. This fit used phase shifts calculated using a common interstitial potential and which included Hedin–Lundqvist excited state contributions, calculated using the default value of 1.325 eV for the inverse lifetime of the core hole. An overall amplitude factor (AFAC) of 1, was used throughout. Multiple scattering terms of up to fifth order were included for paths containing up to five different scattering atoms. The maximum pathlength was 11 Å.

Previously we employed the restrained refinement procedure⁴¹ available in EXCURVE to analyse the two model compounds together with the same species in solution. However, by including in the present analysis all the inter-ligand multiple scattering paths and in addition the intra-ligand paths involving bonded atoms, the result obtained using unmodified crystallographic coordinates is so good that we no longer consider this necessary, and we here use the constrained refinement procedure. This involves moving the ligand position and orientation in terms of the distance to and rotation about a pivotal point within the ligand (atom A₁₁ in Fig. 1). This preserves all internal distances, angles and torsion angles within the ligand, whilst allowing those involving the central atom to vary. As the ligands in question are bidentate, and have a significant difference between the two metal oxygen distances, we selected a point between the two oxygens as the pivotal point used in refinements. In terms of EXCURVE parameters, this involves creating a 'ghost' atom whose coordinates are defined as the mid-point of the vector R_{O1}–R_{O2}, where R_{O1}, R_{O2} are the starting coordinates, taken from one or other of the model compound

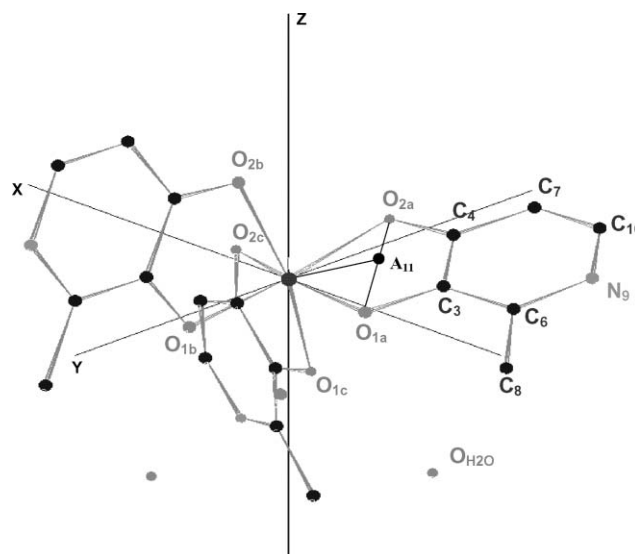


Fig. 1 Structure of Fe(dmpp)₃ showing the terminology used. A₁₁ is the 'ghost' atom.

structures as deduced by X-ray crystallography (Fig. 1). The angles β and $180^\circ - \beta$ subtended at the ghost atom are defined as e.g. $\beta_{0-1-1} = \text{angle}(\text{Fe}-\text{A}_{11}-\text{O}_{1a})$; $\beta = 90^\circ$ when the two oxygen distances are equal.

In the absence of restraints, the number of refinable parameters in the EXAFS analysis is limited to about 10 parameters, and we prefer to use rather fewer than this as some are strongly correlated. This limited the complexity of the analysis. The model compound $\text{Fe}(\text{dmpp})_3$ was admirable in that it has three identical bidentate ligands, plus a hydration nearest shell of three water molecules at 4.2 Å. It was therefore possible to analyse the pyridinone complexes using crystallographic data as a starting model, and refining just the ligand and water distances, plus a single rotational angle. The fit to the EXAFS of $\text{Fe}(\text{ma})_3$ was excellent when the published atomic positions was used, but the structure consisted of three significantly different ligands at slightly different distances. It was therefore necessary to devise a simpler model for the pyranone complexes. The best model was found to be one in which the nitrogen in the pyridinone was replaced by an oxygen, and this proved superior to either the use of an averaged or a single pyranone group taken from the structure of $\text{Fe}(\text{ma})_3$. When considering the significance of the solvent shells, it is necessary to be rigorous in applying statistical criteria to the fitting procedure. For this reason, whenever the χ^2 values, ϵ_v^2 are quoted, we used an experimental measure of data noise. This was obtained from a ten-point moving average of the absolute value of the difference between the EXAFS function and a wide-window back transform (a function which is available automatically in EXCURVE). This not only includes statistical noise, but the discrepancy in background subtraction and in treatment of atomic effects that will normally be greater than random effects for small-molecule data. Our approach thereby involves a pessimistic evaluation of the data. The χ^2 function is described by Lytle *et al.*⁵⁶

$$\epsilon_v^2 = 1/(N_{\text{ind}} - p)(N_{\text{ind}}/N) \sum_i^N W_i (\chi_i^{\text{exp}}(k) - \chi_i^{\text{th}}(k))^2 \quad (1)$$

where N_{ind} is the number of independent data points and p the number of parameters. N_{ind} is normally less than the number of data points N , and in the case that the data from k_{min} to k_{max} are Fourier filtered using a window r_{min} to r_{max} it is given by:

$$N_i = 2(r_{\text{max}} - r_{\text{min}})(k_{\text{max}} - k_{\text{min}})/\pi \quad (2)$$

r_{min} and r_{max} should indicate the range in r -space actually fitted, not just that where structure is apparent. The variable p should include all parameters refined at any time, not just those included in the last refinement. In the program, N_{ind} is calculated automatically, but may be overridden if the automatic value is inappropriate. The parameter p must always be entered by the user. Both these parameters should be quoted and justified along with χ^2 if changes in χ^2 are to be used as evidence for a fit. The absolute value of χ^2 is not meaningful, unless actual experimental statistical errors σ_i have been read-in, and used to weight the spectra.

The overall quality of fit can be described by the R factor:

$$R_{\text{EXAFS}} = \sum_i^N 1/\sigma_i (|\chi_i^{\text{exp}}(k) - \chi_i^{\text{th}}(k)|) \times 100\% \quad (3)$$

and gives a meaningful indication of the quality of fit to the EXAFS data in k -space. A value of around 20% would normally be considered a reasonable fit, with values of 10% or less being difficult to obtain on unfiltered data.

In the present work the values obtained for the R factor, which are presented in Tables 2–4 are smaller than 20% for the solid samples, with the exception of the most lipophilic compound for which the value is 26% which is still reasonable for data obtained at room temperature. For the solution samples the R factors are in the range 16–26% and we believe that the main reason for such a difference is the different solubility of the compounds. We used the same solvent mixture for all the compounds and in fact we did notice that for $\text{Fe}(\text{dmpp})_3$, which is the most soluble compound the value obtained for the R factor (16.00) is quite good for solution.

Table 2 Best fit parameters and (variances) for Fe(III) pyranonate and alkyl pyridinonate complexes^a

	Pyranones				Alkyl pyridinones		
	Fe(ma) ₃ solid	Fe(ma) ₃ solution	Fe(etma) ₃ solid	Fe(etma) ₃ solution	Fe(dmpp) ₃ solid	Fe(dmpp) ₃ solution	Fe(mpp) ₃ solid
E_r	−3.83 (0.30)	−3.32 (0.53)	−3.54 (0.34)	−4.17 (0.42)	−5.12 (0.22)	−4.08 (0.32)	−3.68 (0.34)
R_{11}	1.53 (0.00)	1.53 (0.01)	1.53 (0.00)	1.54 (0.01)	1.56 (0.00)	1.54 (0.00)	1.54 (0.00)
R_1	1.96 [2.00]	1.98	1.97	1.98	1.98 [1.99]	1.98	1.98
R_2	2.07 [2.07]	2.06	2.06	2.06	2.08 [2.04]	2.07	2.06
R_3	2.78 [2.77]	2.78	2.78	2.79	2.80 [2.79]	2.79	2.79
R_4	2.80 [2.77]	2.80	2.80	2.80	2.82 [2.80]	2.80	2.80
R_6	4.13 [4.12]	4.14	4.13	4.14	4.15 [4.15]	4.14	4.14
R_7	4.20 [4.20]	4.20	4.20	4.20	4.22 [4.19]	4.21	4.20
R_8	4.84	4.85	4.84	4.85	4.86	4.85	4.86
R_9	5.12	5.13	5.12	5.13	5.14	5.13	5.13
R_{10}	5.14	5.14	5.13	5.14	5.16	5.14	5.14
β_{0-1-1}	86.9 (0.2)	87.6 (0.0)	87.4 (0.8)	87.5 (0.3)	87.2 (0.2)	87.4 (0.2)	87.7 (0.7)
a_1	0.010 (0.000)	0.014 (0.000)	0.013 (0.003)	0.010 (0.000)	0.007 (0.000)	0.006 (0.000)	0.008 (0.002)
a_3	0.011 (0.000)	0.011 (0.002)	0.010 (0.000)	0.010 (0.002)	0.010 (0.000)	0.009 (0.001)	0.011 (0.001)
a_6	0.020 (0.003)	0.029 (0.006)	0.017 (0.003)	0.020 (0.002)	0.018 (0.005)	0.017 (0.003)	0.021 (0.002)
$R(\text{EXAFS})$	19.07	26.61	17.15	22.00	16.32	16.00	16.88
ϵ_v^2	0.03	0.05	0.03	0.04	0.05	0.05	0.04

^a E_r is the edge position relative to the photoelectron wave vector; R_n and a_n refer to the distances (in Å) and Debye–Waller terms (in 2Å^2) for shell n ; $R(\text{EXAFS})$, ϵ_v^2 and β are defined in the text. R_n refers to the shell containing atoms O_n , C_n and N_n in Fig. 1. The values inside the square brackets are from the crystallographic data.^{54,55} The values inside the normal brackets are the errors associated with the Debye–Waller terms.

Table 3 Best fit parameters and (variances) for Fe(III) phenyl pyridinonate complexes^a

	Phenyl pyridinones					
	Fe(ppp) ₃ solid	Fe(ppp) ₃ solution	Fe(eptpp) ₃ solid	Fe(pbpp) ₃ solid	Fe(epbpb) ₃ solid	Fe(phpp) ₃ solid
<i>E_f</i>	-4.71 (0.39)	-4.27 (0.39)	-4.43 (0.32)	-4.47 (0.35)	-4.16 (0.39)	-4.09 (0.39)
<i>R</i> ₁₁	1.54 (0.01)	1.54 (0.00)	1.54 (0.00)	1.54 (0.01)	1.54 (0.01)	1.54 (0.01)
<i>R</i> ₁	1.97	1.98	1.98	1.98	1.98	1.98
<i>R</i> ₂	2.07	2.06	2.07	2.06	2.06	2.06
<i>R</i> ₃	2.78	2.79	2.79	2.78	2.78	2.78
<i>R</i> ₄	2.80	2.80	2.81	2.80	2.80	2.80
<i>R</i> ₆	4.14	4.14	4.14	4.14	4.14	4.14
<i>R</i> ₇	4.21	4.20	4.21	4.20	4.20	4.20
<i>R</i> ₈	4.85	4.85	4.85	4.85	4.85	4.85
<i>R</i> ₉	5.13	5.13	5.13	5.13	5.13	5.13
<i>R</i> ₁₀	5.14	5.14	5.15	5.14	5.14	5.14
<i>β</i> ₀₋₁₋₁	87.3 (0.6)	87.5 (0.4)	87.4 (0.4)	87.5 (0.8)	87.6 (0.2)	87.5 (0.0)
<i>a</i> ₁	0.007 (0.002)	0.008 (0.001)	0.007 (0.001)	0.007 (0.002)	0.008 (0.000)	0.008 (0.000)
<i>a</i> ₃	0.010 (0.002)	0.013 (0.003)	0.012 (0.002)	0.011 (0.001)	0.012 (0.001)	0.011 (0.002)
<i>a</i> ₆	0.018 (0.006)	0.015 (0.004)	0.019 (0.004)	0.021 (0.005)	0.026 (0.002)	0.020 (0.005)
<i>R</i> (EXAFS)	19.98	25.51	19.22	18.99	18.59	19.21
<i>ε_v</i> ²	0.05	0.05	0.05	0.09	0.11	0.09

^a *E_f* is the edge position relative to the photoelectron wavevector; *R_n* and *a_n* refer to the distances (in Å) and Debye–Waller terms (in 2 Å²) for shell *n*; *R*(exafs), *ε_v*² and *β* are defined in the text. *R_n* refers to the shell containing atoms *O_n*, *C_n* and *N_n* in Fig. 1. The values inside the normal brackets are the errors associated with the Debye–Waller terms.

Table 4 Best fit parameters and (variances) for Fe(III) benzyl pyridinonate complexes^a

	Benzyl pyridinones		
	Fe(etbpb) ₃	Fe(efbpb) ₃	Fe(embpb) ₃
<i>E_f</i>	-4.16 (0.40)	-4.60 (0.35)	-4.78 (0.50)
<i>R</i> ₁₁	1.54 (0.00)	1.54 (0.00)	1.54 (0.01)
<i>R</i> ₁	2.00	1.98	1.99
<i>R</i> ₂	2.05	2.06	2.06
<i>R</i> ₃	2.80	2.78	2.79
<i>R</i> ₄	2.80	2.80	2.80
<i>R</i> ₆	4.15	4.14	4.15
<i>R</i> ₇	4.20	4.20	4.20
<i>R</i> ₈	4.87	4.85	4.86
<i>R</i> ₉	5.14	5.13	5.13
<i>R</i> ₁₀	5.14	5.14	5.14
<i>β</i> ₀₋₁₋₁	88.5 (0.5)	87.8 (1.0)	87.9 (1.3)
<i>a</i> ₁	0.008 (0.000)	0.007 (0.003)	0.009 (0.003)
<i>a</i> ₃	0.010 (0.002)	0.010 (0.002)	0.016 (0.004)
<i>a</i> ₆	0.016 (0.004)	0.022 (0.004)	0.040 (0.000)
<i>R</i> (EXAFS)	20.49	19.49	26.19
<i>ε_v</i> ²	0.05	0.06	0.05

^a *E_f* is the edge position relative to the photoelectron wavevector; *R_n* and *a_n* refer to the distances (in Å) and Debye–Waller terms (in 2 Å²) for shell *n*; *R*(EXAFS), *ε_v*² and *β* are defined in the text. *R_n* refers to the shell containing atoms *O_n*, *C_n* and *N_n* in Fig. 1. The values inside the normal brackets are the errors associated with the Debye–Waller terms.

Results and discussion

Novel iron(III) complexes with a considerable variety of *N*-phenyl- and *N*-benzyl-3-hydroxy-4-pyridinone ligands have been successfully prepared, in 60–75% yields. The compounds have been obtained as deep red–brown powders and were characterized by elemental analysis, mass spectrometry and IR spectroscopy. The elemental analysis results are consistent with the formation of tris chelate complexes with a variable number of crystallization

water molecules, whose number has been confirmed through thermogravimetric analysis measurements. Mass spectra showed the molecular ion [ML₃H]⁺ and fragmentation products [ML₂H]⁺, [MLH]⁺ and [LH]⁺ due to the loss of ligands thus confirming the complexes have been isolated as tris-chelates. The iron isotope pattern could be observed indicating clearly which species were iron-containing.

The IR spectra exhibit the characteristic bands for 3-hydroxy-4-pyridinones (1620, 1560, 1535, 1515 cm⁻¹) with bathochromic shifts imposed by complexation and a broad band in the region 3400–3200 cm⁻¹ due to hydration. Isolation of hydrated complexes has been reported for the majority of metal ion complexes of the 3-hydroxy-4-pyridinone family of ligands.^{52,55–60} It is interesting to point out that although hydration is found in all these new compounds we observe that for those bearing longer tails and which are consequently more lipophilic the number of water molecules decreases. Comparing complexes with alkyl and aryl derivatives of 3-hydroxy-4-pyridinones the number of water molecules is lower for the aryl group and we believe that the long lipophilic tails repel water disfavoring the formation of a large number of hydrogen bonds and so preventing the formation of hexagonal channels as in alkyl analogues.

Taking into account the applications that we foresee for the ligands studied in the present work and the fact that paramagnetic iron(III) complexes have limited spectroscopic signatures we believe that the structural information obtained both in the solid and solution, is more valuable for the characterization of the present compounds than a more extensive spectroscopic study.

Structural information around the metal centre of the new compounds was obtained by EXAFS as most of the complexes are not likely to crystallize. The results obtained for all complexes exhibit a common pattern which can be seen from the *k*³ weighted Fe K-edge EXAFS and Fourier transform spectra of representative compounds presented in Fig. 2–4.

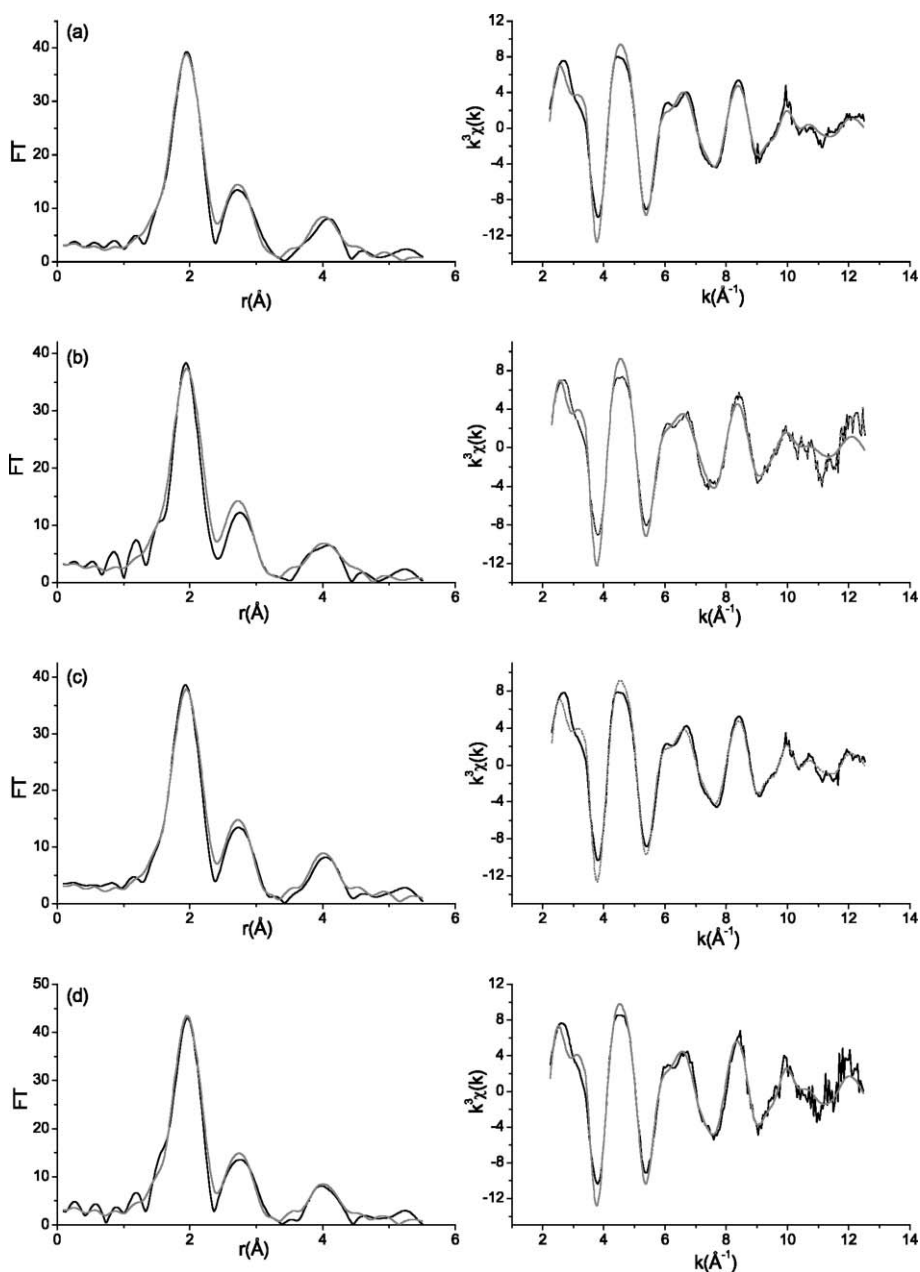


Fig. 2 Fourier transform (left) and best theoretical fit (right) for: (a) $\text{Fe}(\text{ma})_3$, solid, (b) $\text{Fe}(\text{ma})_3$, solution, (c) $\text{Fe}(\text{etma})_3$, solid, (d) $\text{Fe}(\text{etma})_3$, solution. The black line is the experimental; the grey line is the theory.

In all spectra three peaks centred at about 2, 2.8 and 4 Å are clearly seen in the FT spectrum and these correspond to the various shells of atoms detected around the metal centre. The results obtained for all the compounds studied are reported in Tables 2–4.

The distances between the metal centre and the ligand atoms are similar for all the compounds and their average structure may be described as: three oxygen atoms at 1.98 Å, three oxygen atoms at 2.06 Å, three nitrogen or oxygen atoms at 5.13 Å, and shells of three carbon atoms at 2.79, 2.80, 4.14, 4.20, 4.86 and 5.14 Å. It is noticeable that there is a difference of *ca.* 0.08–0.10 Å between the two Fe–O distances of each of the bidentate ligands, as has been

observed for $\text{Fe}(\text{dmpp})_3$, as it is also evident from the values of the angle β obtained for the best fit for each compound.

The values reported in Tables 2–4 do not include the presence of water molecules although the model compound, $\text{Fe}(\text{dmpp})_3$, contained a shell of three water molecules at 4.21 Å. Its inclusion in the calculation improved the fit, and was statistically significant when the shell was described by two parameters (distance + Debye–Waller factor). Including a shell in the pyridinone complexes also improved the fit and appeared significant. However, modelling the water in this way makes the assumption that a single shell of three water molecules is present in the structure. Although it is likely that water is present, (the number of water molecules in the new

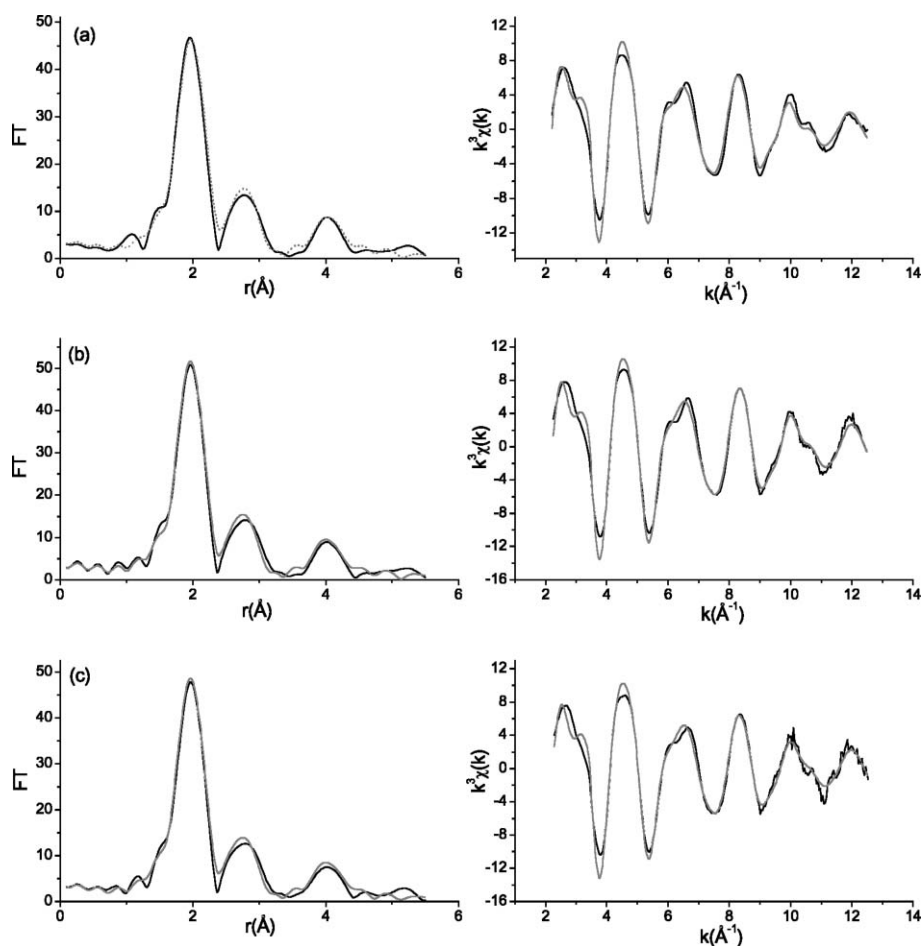


Fig. 3 Fourier transform (left) and best theoretical fit (right) for: (a) $\text{Fe}(\text{dmpp})_3$ solid, (b) $\text{Fe}(\text{dmpp})_3$ solution, (c) $\text{Fe}(\text{mpp})_3$ solid. The black line is the experimental; the grey line is the theory.

compounds varies between one and three), EXAFS is unable to resolve more complex models, and the results presented are based on k^3 weighted refinements that exclude water.

Analysis of the set of MS pathways and their weighted contributions, indicates that the MS pathways that are more significant to the amplitude of the long distance peak at 4 Å are those involving atoms $\text{Fe}-\text{C}_4-\text{C}_7$ and $\text{Fe}-\text{C}_3-\text{C}_6$ in each unit and those through the central atom $\text{O}_1-\text{Fe}-\text{O}_{2a}$ involving two units. For the tris chelates considered in this work the importance of the latter contribution is expected since the $\text{O}_1-\text{Fe}-\text{O}_{2a}$ angles (O_1 and O_{2a} being oxygen donor atoms of different ligands) observed in the model compounds are close to 170° .⁴² The presence of these contributions shows that information on solvation shells is limited by the geometry of the complexes, in particular for those compounds in which ring ligands are present. Comparison of these results with those to be obtained in a parallel study on bis chelates with ligands of the same class should shed more light onto this interesting problem.

Conclusions

All the solid iron(III) compounds have very similar local structure providing a pseudo-octahedral environment around the metal

centre that is not significantly changed by the lipophilicity, bulkiness, or electron-donating or -withdrawing properties of the ligands. This result implies that the lipophilicity of the ligands can be almost freely adjusted in order to get the ligand with the most appropriate properties for the extraction process without losing its strong chelating properties. EXAFS has also been used to analyze some of the compounds in solution. All the complexes are soluble in alcohols and alcohol-water mixtures, but are sparingly soluble or insoluble in water and the structure in solution was evaluated for methanol-water (20 : 80% (v/v)) saturated solutions of the compounds $\text{Fe}(\text{ma})_3$, $\text{Fe}(\text{etma})_3$, $\text{Fe}(\text{dmpp})_3$ and $\text{Fe}(\text{ppp})_3$.

The results obtained and that are reported in Tables 2–4 reveal that the solid state structure is maintained in solution thus confirming the stability of the complexes in such solvents. Further evidence of the similarity of the group of compounds is seen in the edge region of the XAFS spectra. A small ‘pre-edge’ feature, typical of a distorted octahedral environment for a K-edge, is present in each spectrum. The position varies slightly, most notably in the gap between the feature and the main edge is reduced in the solution, consistent with their more ‘molecular’ nature (there is a greater lowering of the interstitial potential in solids).

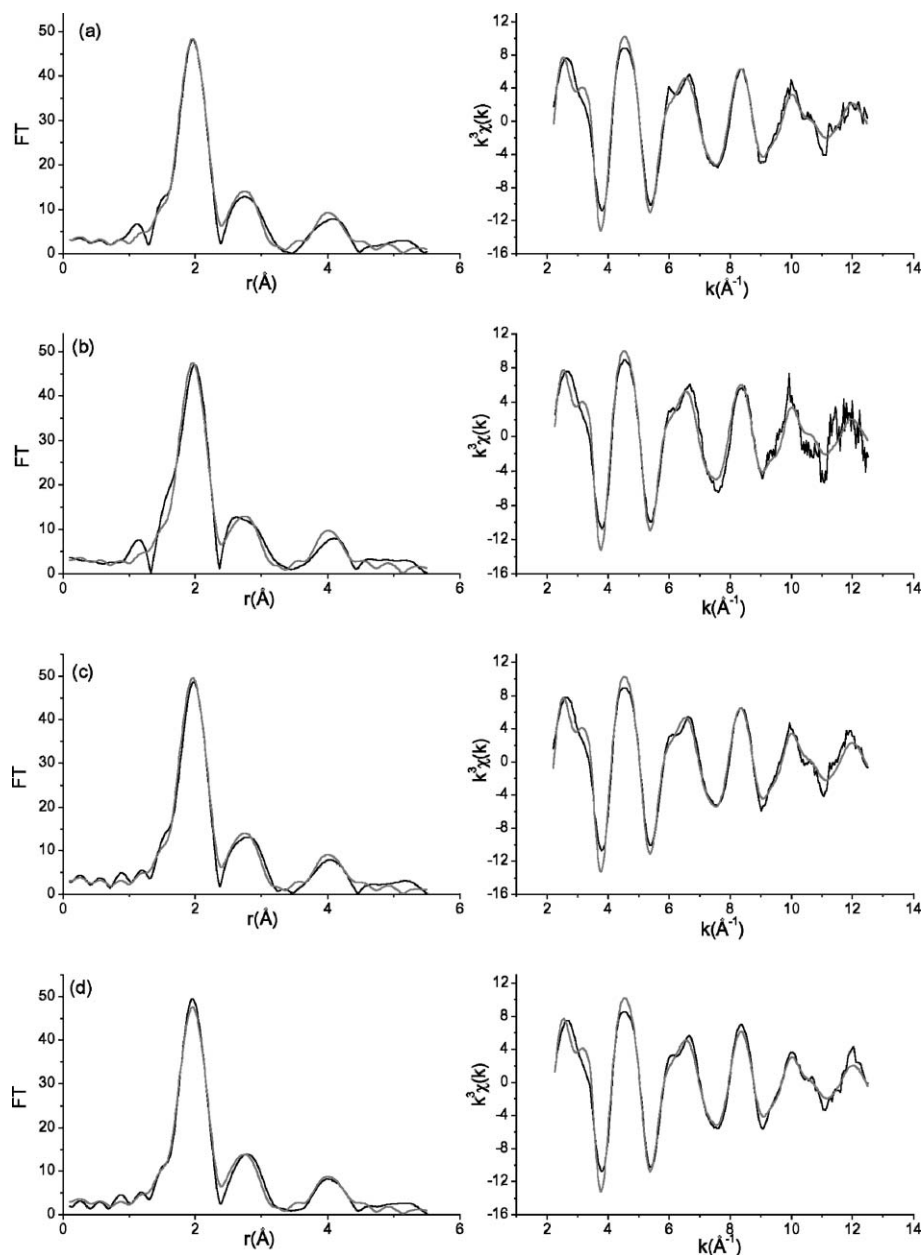


Fig. 4 Fourier transform (left) and best theoretical fit (right) for: (a) $\text{Fe}(\text{ppp})_3$ solid, (b) $\text{Fe}(\text{ppp})_3$ solution, (c) $\text{Fe}(\text{pbpp})_3$ solid, (d) $\text{Fe}(\text{phpp})_3$ solid. The black line is the experimental; the grey line is the theory.

Acknowledgements

Financial support from De Montfort University, The British Council and Fundação para a Ciência e Tecnologia, project POCTI/QUI/56214/2004 is gratefully acknowledged.

References

- 1 R. C. Hider and A. D. Hall, *Prog. Med. Chem.*, 1991, **28**, 41–173.
- 2 J. B. Porter, B. L. C. Gyparakis, E. R. Huehns, P. Sarpong, V. Saez and R. C. Hider, *Blood*, 1988, **72**, 1497–1503.
- 3 J. B. Porter, E. R. Huehns and R. C. Hider, *Baillière's Clin. Haematol.*, 1989, **2**, 257–292.
- 4 J. B. Porter, R. C. Hider and E. R. Huehns, *Sem. Hematol.*, 1990, **27**, 95–100.
- 5 P. S. Dobbin, R. C. Hider, A. D. Hall, P. D. Taylor, P. Sarpong, J. B. Porter, G. Xiao and D. van der Helm, *J. Med. Chem.*, 1993, **36**, 2448–2458.
- 6 G. Stearns and D. Stringer, *J. Nutr.*, 1937, **13**, 127–141.
- 7 E. M. Widdowson and R. A. McCance, *J. Hyg.*, 1936, **36**, 13–23.
- 8 Z. H. Zhang, P. M. Lyster, G. A. Webb and C. Orvig, *Nucl. Med. Biol.*, 1992, **19**, 327–335.
- 9 J. Burgess, *Transition Met. Chem.*, 1993, **18**, 439–448.
- 10 M. J. Clarke, F. Zu and D. R. Frasca, *Chem. Rev.*, 1999, **99**, 2511–2533.
- 11 C. J. Anderson and M. J. Welch, *Chem. Rev.*, 1999, **99**, 2219–2234.
- 12 R. B. Lauffer, *Chem. Rev.*, 1987, **87**, 901–927.
- 13 P. Caravan, J. J. Ellison, T. J. McMurry and R. B. Lauffer, *Chem. Rev.*, 1999, **99**, 2293–2352.
- 14 K. H. Thompson, J. H. McNeill and C. Orvig, *Chem. Rev.*, 1999, **99**, 2561–2571.
- 15 J. Burgess, B. de Castro, C. Oliveira, M. Rangel and W. Schlindwein, *Polyhedron*, 1997, **16**, 789–794.

- 16 M. Rangel, *Transition Met. Chem.*, 2001, **26**, 219–223.
- 17 M. Rangel, A. Tamura, C. Fukushima and H. Sakurai, *J. Biol. Inorg. Chem.*, 2001, **6**, 128–132.
- 18 Y. Yoshihawa, E. Ueda, K. Kawabe, H. Miyake, H. Sakurai and Y. Kojima, *Chem. Lett.*, 2000, 874–875.
- 19 I. Pashalidis and G. J. Kontoghiorghes, *J. Radioanal. Nucl. Chem.*, 1999, **242**, 181–184.
- 20 J. Arnarp, J. Bielawski, B.-M. Dahlin, O. Dahlman, C. R. Enzell and T. Pettersson, *Acta Chem. Scand.*, 1990, **44**, 916–926.
- 21 *Calculation of Drug Lipophilicity*, ed. R. F. Rekker and R. Mannhold, VCH, Weinheim, 1992.
- 22 G. J. Kontoghiorghes and A. May, *Biol. Met.*, 1990, **3**, 183–187.
- 23 B. L. Rai, L. S. Dekho, H. Khodr, Y. Jin, Z. D. Liu and R. C. Hider, *J. Med. Chem.*, 1998, **41**, 3347–3359.
- 24 J. J. Molenda, M. M. Jones and M. A. Basinger, *J. Med. Chem.*, 1994, **37**, 93–98.
- 25 S. Alshehri, J. Burgess and A. Shaker, *Transition Met. Chem.*, 1998, **23**, 689–691.
- 26 M. J. Herak, M. Janko and B. Tamhina, *Mikrochim. Acta*, 1973, **45**, 783–795.
- 27 B. Tamhina and M. J. Herak, *Croat. Chem. Acta*, 1973, **45**, 603–610.
- 28 B. Tamhina and V. Vojkovic, *Mikrochim. Acta*, 1986, **4**, 137–147.
- 29 V. Vojkovic, B. Tamhina and M. J. Herak, *Fresenius' Z. Anal. Chem.*, 1975, **276**, 377–378.
- 30 A. G. Ivsic and B. Tamhina, *Talanta*, 1991, **38**, 1403–1407.
- 31 B. Tamhina, M. J. Herak and K. Jakop, *J. Less-Common Met.*, 1973, **33**, 289–294.
- 32 M. J. Herak and B. Tamhina, *Croat. Chem. Acta*, 1973, **45**, 237–241.
- 33 V. Vojkovic and B. Tamhina, *Solvent Extr. Ion Exch.*, 1986, **4**, 27–39.
- 34 V. Vojkovic and B. Tamhina, *Solvent Extr. Ion Exch.*, 1987, **5**, 245–253.
- 35 B. Tamhina, A. Ivsic and A. Gojmerac, *Solvent Extr. Ion Exch.*, 1987, **5**, 909–922.
- 36 V. Vojkovic, A. G. Ivsic and B. Tamhina, *Solvent Extr. Ion Exch.*, 1996, **14**, 479–490.
- 37 V. Vojkovic, A. G. Ivsic and B. Tamhina, *Croat. Chem. Acta*, 1997, **70**, 667–677.
- 38 B. Tamhina and M. J. Herak, *J. Inorg. Nucl. Chem.*, 1976, **38**, 1505–1507.
- 39 J. Burgess and M. S. Patel, unpublished work.
- 40 J. Burgess, B. de Castro, C. Oliveira and M. Rangel, *J. Chem. Res. (S)*, 1996, 234–235; J. Burgess, B. de Castro, C. Oliveira and M. Rangel, *J. Chem. Res. (M)*, 1996, 1338–1351.
- 41 W. Schlindwein, M. Rangel and J. Burgess, *J. Synchrotron Radiat.*, 1999, **6**, 579–581.
- 42 N. Binsted, A. van der Gaauw, O. M. Wilkin and N. A. Young, *J. Synchrotron Radiat.*, 1999, **6**, 239.
- 43 H. Sakane, A. Munoz-Páez, S. Diaz-Moreno, J. M. Martínez, R. R. Pappalardo and E. S. Marcos, *J. Am. Chem. Soc.*, 1998, **120**, 10397.
- 44 P. Lindqvist-Reis, A. Munoz-Paez, S. Diaz-Moreno, S. Pattanalk, I. Persson and M. Sandsstrom, *Inorg. Chem.*, 1998, **37**, 6675.
- 45 S. Diaz-Moreno, J. M. Martínez, A. Munoz-Páez, H. Sakane and I. Watanabe, *J. Phys. Chem. A*, 1998, **102**, 7435.
- 46 N. Young, *J. Chem. Soc., Dalton Trans.*, 1996, 249.
- 47 N. Young, *J. Chem. Soc., Dalton Trans.*, 1996, 1275.
- 48 N. Binsted, R. W. Strange and S. S. Hasnain, *Biochemistry*, 1992, **31**, 12117.
- 49 Z. Zhang, S. J. Rettig and C. Orvig, *Inorg. Chem.*, 1991, **30**, 509.
- 50 M. Färber, H. Osiander and T. Severin, *J. Heterocycl. Chem.*, 1994, **31**, 947.
- 51 M. M. Finnegan, S. J. Rettig and C. Orvig, *J. Am. Chem. Soc.*, 1986, **108**, 5033.
- 52 W. O. Nelson, S. J. Rettig and C. Orvig, *Inorg. Chem.*, 1989, **28**, 3153.
- 53 N. Binsted, *PAXAS*, 1996.
- 54 M. T. Ahmet, C. S. Frampton and J. Silver, *J. Chem. Soc., Dalton Trans.*, 1988, 1159.
- 55 E. T. Clarke, A. E. Martell and J. Reibenspies, *Inorg. Chim. Acta*, 1992, **196**, 177.
- 56 F. W. Lytle, D. E. Sayers and A. Stern, *Physica B*, 1989, **158**, 701.
- 57 W. O. Nelson, T. B. Karpishin, S. J. Rettig and C. Orvig, *Can. J. Chem.*, 1987, **66**, 123.
- 58 W. O. Nelson, S. J. Rettig and C. Orvig, *J. Am. Chem. Soc.*, 1987, **109**, 4121.
- 59 C. A. Matsuba, W. O. Nelson, S. J. Rettig and C. Orvig, *Inorg. Chem.*, 1988, **27**, 3935.
- 60 W. O. Nelson, T. B. Karpishin, S. J. Rettig and C. Orvig, *Inorg. Chem.*, 1988, **27**, 1045.